Original paper

Luminescence properties of Ce³⁺ and Eu²⁺ in fluorites and apatites

Sabina BODYŁ[1]

[1] *University of Silesia, Faculty of Earth Sciences, 41-200 Sosnowiec, Będzińska 60, Poland;
e-mail: sbodyl@wnoz.us.edu.pl*

Abstract. Natural samples of fluorite and apatite from granites, pegmatites, carbonatites and andesitic tuffs were investigated by steady-time spectroscopy to characterize the luminescence properties of Ce^{3+} and Eu^{2+}. The luminescence of Ce^{3+} has been clearly seen in fluorite as 320 and 337 or 343 nm bands. In apatites, two distinct bands for two different Ca crystal sites were obtained: 340–380 nm for Ca(1) and 420–450 nm for Ca(2). The luminescence spectra of Eu^{2+} in the fluorite crystals were measured even at for low concentration of this element (0.11 ppm). For Ce^{3+}, it has been showed that the crystal field strength depends more on the nature of the ligand than on the Me-ligand distances.

Key-words: fluorite, apatite, REE, luminescence

1. Introduction

The luminescence of rare earth elements (REE) in fluorite and apatite has been well known for almost sixty years. Different types of luminescent centers have been studied by photoluminescence, cathodoluminescence and X-ray luminescence techniques. For natural fluorites, luminescence spectra have been ascribed to the RE ions Ce^{3+}, Nd^{3+}, Sm^{3+}, Sm^{2+}, Eu^{3+}, Eu^{2+}, Gd^{3+}, Tb^{3+}, Dy^{3+}, Ho^{3+}, Er^{3+}, Tm^{3+} and Yb^{2+} (Aierken et al. 2003; Gaft et al., 2005). In apatites, on the other hand, luminescence due to Ce^{3+}, Pr^{3+}, Nd^{3+}, Sm^{3+}, Eu^{2+}, Eu^{3+}, Tb^{3+}, Dy^{3+}, Ho^{3+}, Tm^{3+} and Yb^{3+} has been observed (Gaft et al. 2001a; Waychunas 2002). These luminescent properties have found many applications, e.g. in the detection and identification of minerals in rocks and ores.

The aim of this paper is to verify the thesis that two non-equivalent crystal sites are occupied by Ce^{3+} ions in apatites and to discuss the effect of the Me-ligand distance and of the nature of the ligand, on the crystal field strength (for apatite and fluorite). Steady-time photoluminescence techniques (emission- and excitation measurements) were used.

2. Fluorite

In fluorite (CaF_2; Fm_3m lattice), the F^- ions are at the center of smaller cubes obtained by dividing the unit cube into eight parts and each is surrounded by four Ca^{2+} ions located at the corners of the regular tetrahedron. The Ca^{2+} ions are coordinated by eight fluorine ions.

In the fluorite crystal structure, REE enter two small, cubic and trigonal sites, with the size 2.365 Å and bigger, tetragonal site (Weber, Bierig 1964).

The cubic (O_h) sites play a role in the simple REE-Ca substitution and the trigonal sites (C_{3v}) for REE situated on <111> axes and with one F^- replaced by O^{2-}. The smaller positions, with a Ca⇔F distance of 2.365 Å are usually occupied by REE ions with smaller ionic radii (from Gd to Yb). The larger tetragonal sites arise from F^- ion displacement to an interstitial position on <100> axes. The Ca⇔F distance for this position is 2.725 Å, convenient for REE ions with larger radii (from Ce to Eu).

3. Apatite

Apatite $Ca_5(PO_4)_3(OH,F,Cl)$ has a hexagonal structure with the symmetry group $P6_3/m$. Several varieties of apatite are known: apatite-(CaF), apatite-(CaCl), apatite (CaOH) and apatite-(SrOH). In the unit cell of apatite-(CaF), which is the model for this group, the following polyhedra occur: three-phosphate tetrahedra [PO_4], a $Ca(1)O_9$ polyhedron and a $Ca(2)O_6F$ polyhedron. The charge compensation process for apatite-(CaF) is as follows (Fleet et al. 1997):

$$REE^{3+} + Si^{4+} = Ca^{2+} + P^{5+}, Ca_{10-x}REE_x(P_{1-x}Si_xO_4)_6A_2 \tag{1}$$

or

$$REE^{3+} + Na^{1+} = 2Ca^{2+}, Ca_{10-2y}Na_yREE_y(PO_4)_6A_2 \tag{2}$$

In apatite-(CaCl), REE substitutions for Ca are compensated by:

$$REE^{3+} + Na^{1+} = 2Ca^{2+}, Ca_{10-2}Na_yREE_y(PO_4)_6A_2 \tag{3}$$

In apatite-(CaOH), the substitutions are compensated by:

$$REE^{3+} + Si^{4+} = Ca^{2+} + P^{5+}, Ca_{10-6x} REE_{6x}(P_{1-X}Si_XO_4)_6A_2 \tag{4}$$

In the apatite structure, two crystal sites with different point symmetries exist which may be occupied by different REE^{2+} or REE^{3+} ions. The point symmetry group of the Ca(1) site is C_3, where each Ca has six oxygen atoms as its nearest neighbors; they form a distorted triangular prism around the Ca^{2+} ion. The second position, Ca(2), has a C_s symmetry with the Ca^{2+} ions present in the corners of equilateral triangles with the F^- ion in their centers. The Me-ligand distances in the apatite structure are: 2.44 Å for Ca(1)$\Leftrightarrow O_6$, and from 2.34 to 2.70 Å for Ca(2)$\Leftrightarrow$(O,F).

3.1. Electronic states of Ce^{3+} ions

Cerium in minerals usually exists in the form of Ce^{3+}. Its valence state reflects the loss of two of its 6s electrons and one of its 4f electrons. The ground state of Ce^{3+} splits into two levels, $^2F_{7/2}$ and $^2F_{5/2}$, usually separated by 2000–3000 cm^{-1}. In the cubic crystal field 5d, the excited state also splits into two levels, T_{2g} and E_g; the energy difference between them is usually termed the crystal field parameter 10Dq (Fig. 1) (Aierken et al. 2000). Absorption and emission bands of electron transitions between the ground and the two excited levels are located in the UV region, between 200 and 305 nm. The emission of Ce^{3+} results from 4f–5d electric-dipole transitions which are parity and spin-allowed and have a large oscillator strength; as a result, the emission bands are very intensive and broad. A further interesting characteristic is the very short luminescence decay time (10^{-7}–10^{-8} s; Gaft et al. 2005). The position of the emission peak depends on the host material (mineral).
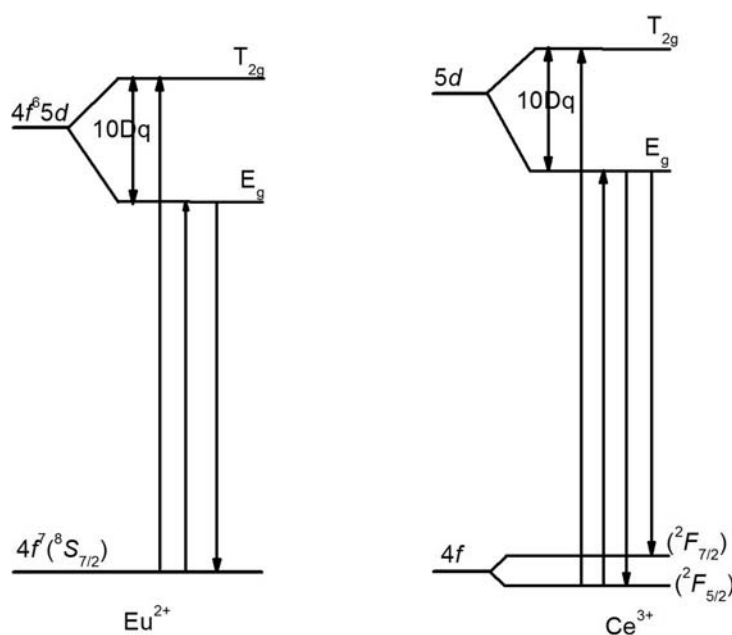

Fig. 1. Scheme Eu^{2+} and Ce^{3+} energy levels in a cubic crystal (T_d crystal symmetry);
the excited level of Ce^{3+} is denoted as $^2D_{3/2,5/2}$
(for O_h symmetry, level E_g has a higher energy than level T_{2g}, Aierken et al. 2000)

3.2. Electronic states of Eu^{2+} ions

In the group of REE^{2+}, Eu^{2+} ions are best known as luminescence centers. Many have published on Eu^{+2} luminescence (e.g. Gaft et al. 1998; Caldino et al. 1989; Gaft et al. 2001a; Aierken et al. 2000, 2003). However, in apatite, Eu^{3+} luminescence is more frequently measured than that of Eu^{2+}. Because the Eu^{2+} and Ce^{3+} emission transitions for apatite lie in the same energy band, Eu^{2+} is usually detected as a shoulder on the Ce^{3+} emission band. If the Eu concentration is lower than that of Ce, the detection of Eu^{2+} ions is almost impossible (Gaft et al. 2005).

The absorption and excitation spectra of Eu^{2+} correspond to transition between the configuration $4f^7$ and $4f^65d^1$; this causes broad absorption/emission bands. The position of emission bands also depends on host materials and varies from near-UV to red. The ground state of Eu^{2+} is $4f^7$ ($^8S_{7/2}$) and the excited state 5d splits into two levels, i.e. T_{2g} and E_g (Fig. 1). The decay time of Eu^{2+} ranges from $6-8 \times 10^{-9}$ s (Gaft et al. 2005).

The luminescence of Eu^{3+} has not been detected in natural fluorite using steady-state spectroscopy; it is caused by the strong emission band of Eu^{2+} (Gaft et al. 2001b). However, in natural apatite-(CaF) crystals, it has been often measured by this method (Reisfeld et al. 1996).

4. Samples and experimental studies

4.1. Samples

In this work, three monocrystals of fluorite and three monocrystals of apatite were studied (Table 1). These, chosen from a large number of samples, are characterized by excellent optical quality and homogeneity. The abundance of RE impurities in the fluorite and apatite is shown in Table 1.

The fluorites contain 12–139 ppm Ce, the apatites 7200–355 ppm. The concentration of Eu is low compared to Ce in all of the samples; the fluorites contain 0.11–14 ppm, the apatites 26–114 ppm.

TABLE 1

The concentration of cerium and europium in the minerals studied

Mineral	Origin (type of rock)	REE [ppm]	
		Ce	Eu
Fluorite (China)	unknown	13.0	0.11
Fluorite (Russia – Transbaical region)	granite	12.0	10.0
Fluorite (Poland – Tajno)	carbonatite	139	14.0
Apatite (Spain) (apatite-(CaOH))	andesitic tuff	7200	114
Apatite (S. Africa) (apatite-(CaOH))	carbonatite	355	26.0
Apatite (Morocco) (apatite-(CaOH))	pegmatite	5450	48.0

4.2. Experimental

The steady-state luminescence measurements were performed with a Fluorolog FL3-12 (Spex-Jobin-Yvon) spectrofluorimeter equipped with a 450 W xenon lamp, single-grating excitation monochromator and a double-grating emission monochromator and a photomultiplier (type R928). The radial sensitivity of this photomultiplier is the same over the whole measurement spectral range. The excitation spectra were recorder in the range 240–400 nm and the emission ones spectra in the range 300–500 nm. All the measurements were carried out at room temperature.

The apatite samples were assessed by RTG diffraction measurements using a Philips PW 3710 diffractometer with Co ká radiation and a graphite monochromator.

The chemical analyses were carried out at the ACME laboratory (Vancouver, Canada) and the concentrations of RE ions were determined using the inductive-coupled plasma (ICP) method.

5. Results and discussion

5.1. Fluorite

The luminescence spectra of the studied fluorites are shown in Figures 2–4. Figure 2 shows the excitation spectrum that consists of a small A band at 305 nm and a complex B band at 337, 353, 366 and 376 and 396 nm. The A band at 305 nm is the transition between the lower excited state 5d (E_g) and ground state 4f ($^2F_{5/2}$) of the Ce^{3+} ions. Several authors have previously
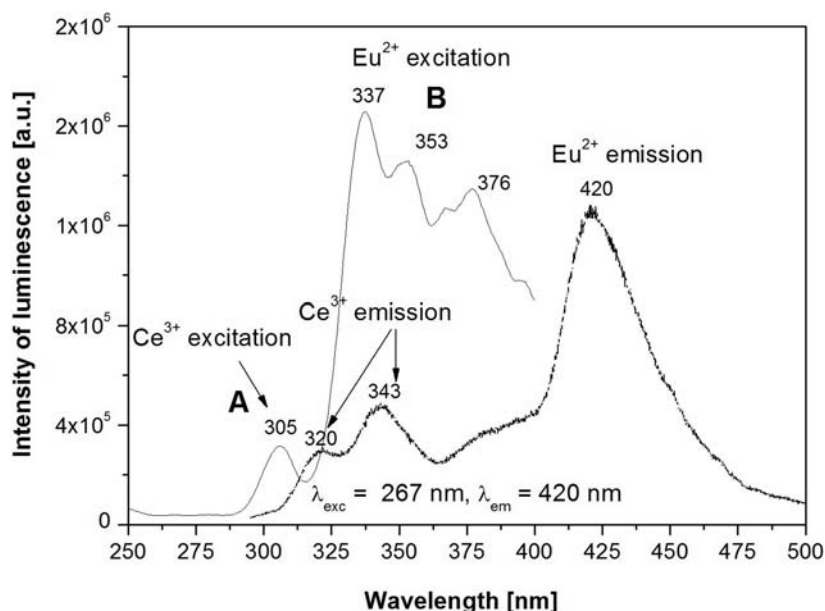

Fig. 2. The emission and excitation spectra of Ce^{3+} and Eu^{2+} in the Chinese fluorite (Table 1)

reported a band at about 220–260 nm (Caldino et al. 1989; Aierken et al. 2000, 2003) corresponding to the Ce^{3+} transition $4f \rightarrow {}^2T_g$ (5d); this was not possible to measure with our equipment. The Ce^{3+} emissions were obtained for $\lambda_{exc} = 267$, 295 and 306 nm while, for $\lambda_{exc} = 306$ nm, two emission bands with maxima at 320 (Fig. 3) and at about 337 (343) nm (Fig. 2 and 3) were
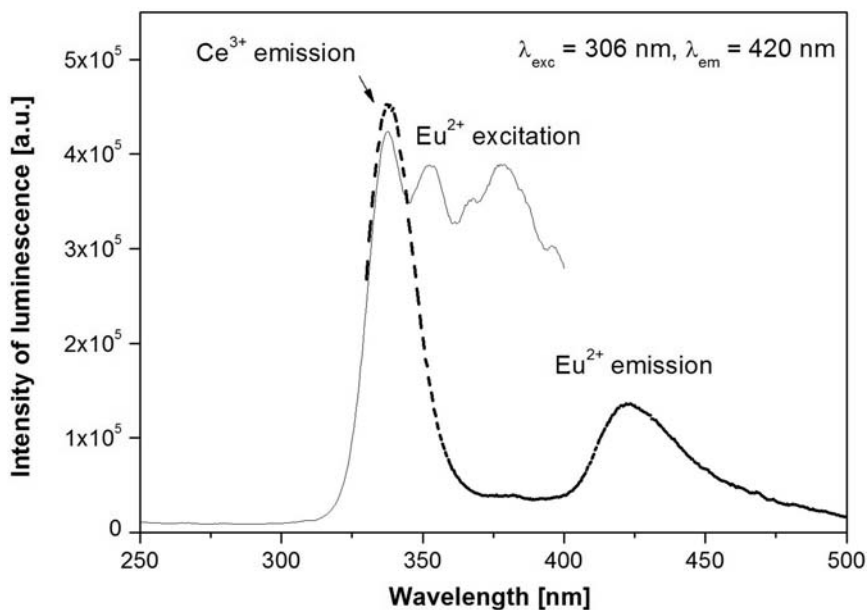

Fig. 3. The emission and excitation spectra of Ce^{3+} and Eu^{2+} in the Russian fluorite (Table 1)
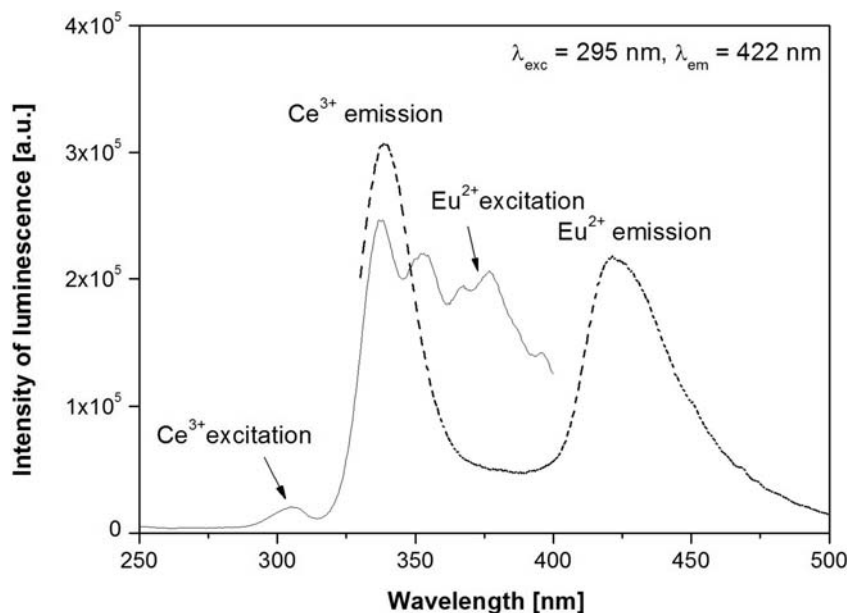

Fig. 4. The emission and excitation spectra of Ce^{3+} and Eu^{2+} in the Polish fluorite (Table 1)

measured which are the electronic transitions between 5d (E_g) $^2D_{3/2,5/2}$ and 4f ($^2F_{5/2}$, $^2F_{7/2}$) levels for Ce^{3+} (Arieken et al. 2000) and $^2F_{5/2}$–$^2F_{7/2}$ splitting is 2094 cm^{-1}.

The complex B band is attributed to the electronic transition from the ground state $4f^7$ ($^8S_{7/2}$) to the lower excited state $4f^65d$ (E_g) of Eu^{2+}. The complex nature of this transition is due to fact that the excitation state is split into seven states $4f^6$ (^7F_J) 5d with a total angular momentum $J = 0$–6, though a few transitions to sublevels $J = 0$, 1 and 2 do not appear at room temperature (Aierken et al. 2000). The emission spectra of Eu^{2+} measured at $\lambda_{exc} = 267$ nm (Fig. 2), 306 nm (Fig. 3) and at 295 nm (Fig. 4) as a broad band while a band measured at $\lambda_{exc} = 337$ was the most intensive. Such a spectrum was reported in the literature for both natural and synthetic CaF_2 crystals. This band was attributed to the electronic transition from the lower excited state $4f^65d$ (E_g) to the ground state $4f^7$ ($^8S_{7/2}$) of Eu^{2+}.

In all of the fluorite luminescence spectra (Fig. 2, 3 and 4), there is a partial overlap of the emission band of Ce^{3+} (337–343 nm) and the short-wavelength part of the B excitation band of Eu^{2+}. Thus, Ce $\rightarrow$ Eu energy transfer is likely.

5.2. Apatite

Figures 5–7 show the luminescence spectra of the natural apatites. The emission spectra of Ce^{3+} were detected as broad complex bands (Fig. 5 and 7) at 370 and 420 nm. The most intensive emission bands were received for $\lambda_{exc} = 302$–320 nm and at 265 nm according to the excitation spectra (Fig. 5–7). These two emission bands reflect the presence of RE ions at two different sites in the apatite crystal structure. For Ce^{3+} ions in the higher point-symmetry Ca(1) sites, emission bands occur in the range 340–388 nm. These emission bands are complex with some shoulders at 340–348 nm on the main peak at 364–388 nm. These can be explained as reflecting electronic
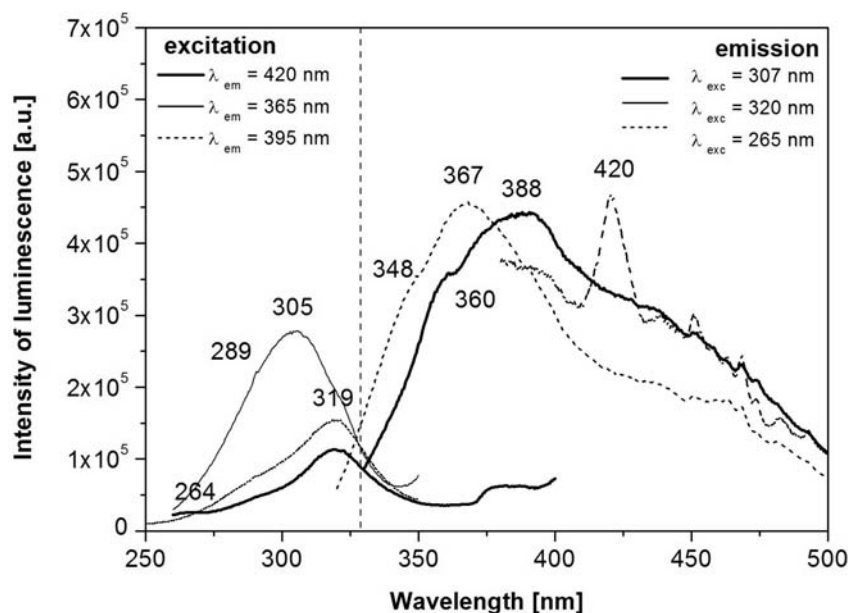

Fig. 5. The excitation and emission spectra of Ce^{3+} in the Spanish apatite (Table 1)
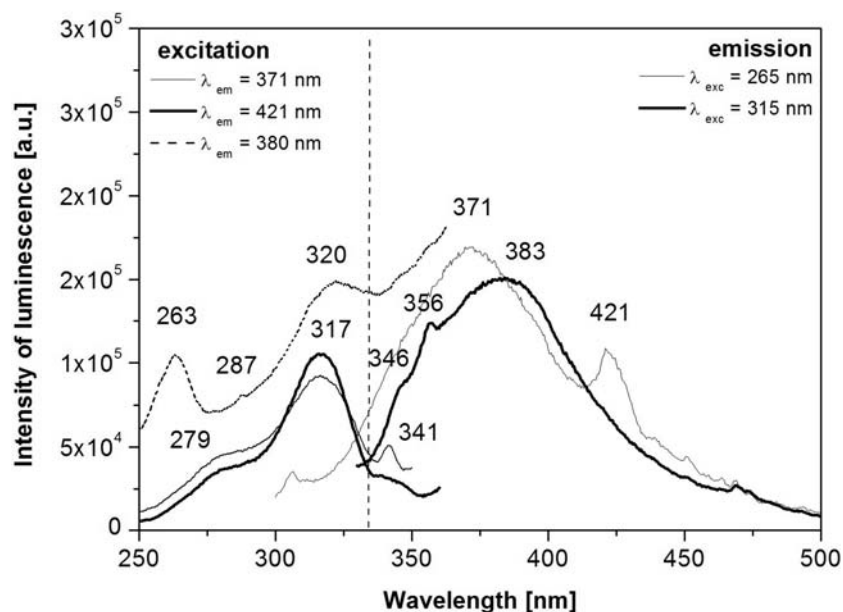
Fig. 6. The excitation and emission spectra of Ce^{3+} in the South African apatite (Table 1)
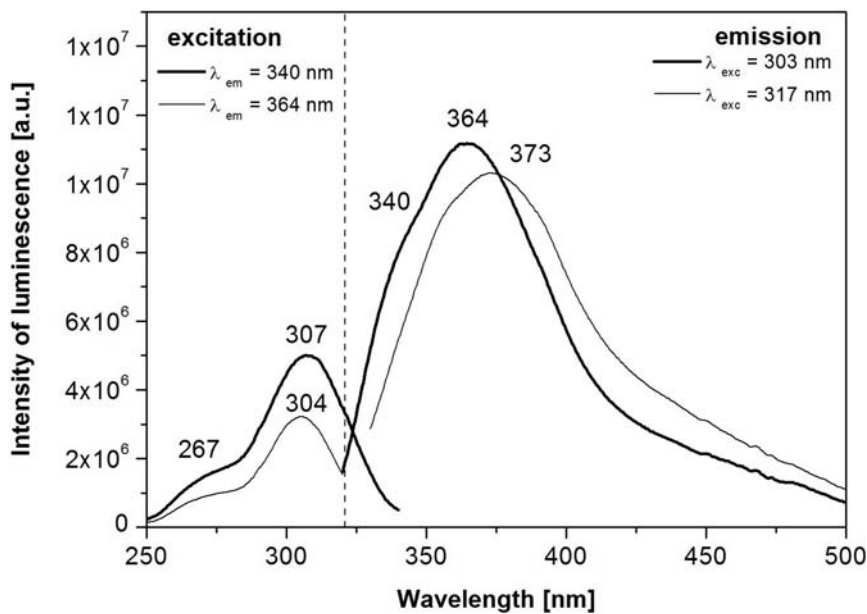

Fig. 7. The excitation and emission spectra of Ce^{3+} in the Moroccan apatite (Table 1)

transitions between the levels 5d (T_g) $^2D_{3/2,5/2}$ and 4f ($^2F_{5/2}$, $^2F_{7/2}$) for Ce^{3+}. (Note: for the nd electrons of an ion being in the O_h point symmetry or its subgroup, e.g. C_3, the T_g level has lower energy than E_g). The energy gap between the $^2F_{5/2}$ and $^2F_{7/2}$ levels, different for each apatite

crystal, falls in the range 1488–2790 cm^{-1}. The emission of the Ce^{3+} ions occupying the Ca(2) sites was measured for λ_{exc} = 265 nm as a band at 420–450 nm. The difference in the REE-O distances for the two Ca various crystal sites is the reason for the differences in the crystal field strength and, as a consequence, the different splitting between ground- and excited levels.

The emission of Eu^{2+} in apatite crystals has not been obtained using the steady-time technique. Only can time-resolved measurements differentiate luminescence centers with different decay times – longer for Eu^{2+}, shorter for Ce^{3+}. The emission of Eu^{2+} was obtained at 420–450 nm by Gaft et al. (2001a). Thus, for the steady-time spectra presented in this paper, the Eu^{2+} emission can be only presumed to be a weak shoulder on the Ce^{3+} luminescence band at 420–450 nm. For these apatites, as the distinct emission spectra of Eu^{3+} ions were measured, the presence of europium as Eu^{3+} is indicated.

The energy gap between energy the energy levels 4f–5d for Ce^{3+} in the samples could be determined from the values of the emission energies. In the emission spectra of Ce^{3+} in fluorite and apatite, the maximum emissions are different. For fluorites, the energy gap between 4f and 5d levels is greater than for the apatites. For the fluorites, λ_{em} = 320–340 nm can be expressed in [eV] energy units as 3.85 and 3.63 eV and λ_{em}= 420 nm as 2.94 eV according to the relation E [eV] = 1234/λ [nm]. For the apatites, λ_{em} = 340–380 nm can be likewise expressed as 3.63 and 3.25 eV and λ_{em}= 420 nm as 2.94 eV. The value of the energy gap between the 4f and 5d levels depends on the Me-ligand distance, the coordination number and the nature of the ligand.

1. Dependence on Ce^{3+}-ligand distances:
   a) The Ca(1)⇔O distance in apatite is close to the Ca⇔O distance in scheelite (2.4811 and 2.4362 Å, respectively) for which λ_{em} of Ce^{3+} is equal to 355 nm or 3.48 eV (Gaft et al. 2001a) and is in the range of Ce^{3+} emission from the Ca(1) site of apatite.
   b) As the Ca⇔F distance in fluorite (2.3655 Å) is shorter than Ca⇔O distance in apatite, it is evident that for the shorter Me-ligand distance, the energy gap is significantly greater.
2. Dependence on the nature of ligand:
   The emission spectra of the Ce^{3+} ions in fluorites were compared to the emission spectrum on fluoroperovskite KCaF$_3$: Ce^{3+}, Pr^{3+}. In this crystal the Ca⇔F distances are 2.21 and 2.16(9) Å (Ratuszna et al. 1997) and the emission band of Ce^{3+} is at 408 nm (3.02 eV) (Mazurak et al. 1999). Because Δ_{oct} = –8/9 Δ_{cubic}, for the eightfold coordination and Ca⇔F distances as for the fluoroperovskite, the measured emission line should be at 363 nm and, thus, the energy gap should be smaller than for the fluorite. However, the shortest Ce^{3+}-ligand distances apply for the fluoroperovskite (the smallest energy gap was determined for this crystal) and, thus, crystal field strength depends on the nature of ligand more than on Me-ligand distances.

6. Conclusions

The emission bands of cerium ions in the studied minerals are complex, and are explained by electronic transition from the 5d (E$_g$) to 4f (^{2}F$_{5/2}$, ^{2}F$_{7/2}$) states. The emission peak dependence on the nature of the ligand and on Ce^{3+}-ligand distances. For the first time for Ce^{3+} ions, it has been demonstrated that the energy of the excited level depends on the nature of the ligand more than on Me-ligand distances. Furthermore, the occupancy of the two non-equivalent crystal sites by

Ce^{3+} ions was confirmed by attributing the excited level to the correct emission band. The two distinct emission bands show the dependence of the crystal field strength on Ce^{3+}-O distances.

Using steady-state spectroscopy, it is possible to detect very low concentrations of Eu (e.g. in the fluorite from China – 0.11 ppm). However, detecting divalent europium in apatite is almost impossible due to the Eu^{2+} luminescence being in the same spectral range as that of Ce^{3+}.

The emission band of europium in fluorite always takes the same position for every measured sample (420 nm). Its nature has been attributed to the electronic transition from the excited state $4f^6 5d$ (E_g) to the ground state $4f^7$ ($^8S_{7/2}$).

7. References

Aierken S., Lee K.-H., Kusachi I., & Yamashita N. (2000). Photoluminescence properties of natural fluorite. *Journal of Mineralogical and Petrological Sciences*, 95(8), 228–235.

Aierken S., Kusachi I., & Yamashita N. (2003). Natural fluorite emitting yellow fluorescence under UV light. *Physics and Chemistry of Minerals*, 30(8), 478–485. DOI: 10.1007/s00269-003-0341-3.

Caldino U.G., Dela Cruz C., Muhoz G., & Rubio J.O. (1989). Ce^{3+} – > Eu^{2+} energy transfer in CaF_2. *Solid State Communications*, 69 (4), 347–351. DOI: 10.1016/0038-1098(89)90685-6.

Fleet M.E., & Pan Y. (1997). Site preference of rare elements in fluorapatite: Binary (LREE+HREE) – substituted crystals. *American Mineralogist*, 82(9–10), 870–877.

Gaft M., Reisfeld R., Panczer G., Blank PH., & Boulon G. (1998). Laser-induced time-resolved luminescence of minerals. *Spectrochimica Acta Part A*, 54(13), 2163–2175. DOI: 10.1016/S1386-1425(98)00134-6.

Gaft M., Panczer G., Reisfeld R., & Uspersky E. (2001a). Laser induced time-resolved luminescence as a tool for rare-earth element identification in minerals. *Physics and Chemistry of Minerals*, 28(5), 343–363. DOI 10.1007/s002690100163.

Gaft M., Panczer G., Reisfeld R., Ioffe O., & Sigali I. (2001b). Laser induced time-resolved luminescence as a means for discrimination of oxidation states of Eu in minerals. *Journal of Alloys and Compounds*, 323–324, 842–846. DOI: 10.1016/S0925-8388(01)01157-4.

Gaft M., Reisfeld R., & Panczer G. (2005). *Luminescence Spectroscopy of Minerals and Materials*. Berlin: Springer-Verlag.

Mazurak Z., Ratuszna A., & Daniel Ph. (1999). Luminescence properties of Pr^{3+} and Ce^{3+} in $KCaF_3$ single crystals. *Journal of Luminescence*, 82(2), 163–171. DOI: 10.1016/S0022-2313(99)00028-9.

Ratuszna A., Rousseau M., & Daniel Ph. (1997). Crystal structure of $KCaF_3$ determined by Rietveld profile method. *Powder Diffraction*, 12(2), 70–76.

Reisfeld R., Gaft M., Boulon G., Panczer G., & Jorgensen C.K. (1996). Laser-induced luminescence of rare-earth elements in natural fluor-apatites. *Journal of Luminescence*, 69(5–6), 343–353. DOI: 10.1016/S0022-2313(96)00114-7

Waychunas G.A. (2002). Apatite luminescence. Reviews in Mineralogy and Geochemistry, 48(1), 701–742. DOI: 10.2138/rmg.2002.48.19.

Weber J.M., & Bierig R.W. (1964). Paramagnetic Resonance and Relaxation of Trivalent Rare-Earth Ions in Calcium Fluoride. I. Resonance Spectra and Crystal Fields. *Physical Review*, 134(6A), A1492–A1503. DOI: 10.1103/PhysRev.134.A1492.